Mitochondrial Genome of the Homoscleromorph *Oscarella carmela* (Porifera, Demospongiae) Reveals Unexpected Complexity in the Common Ancestor of Sponges and Other Animals

Xiujuan Wang and Dennis V. Lavrov

Department of Ecology, Evolution and Organismal Biology, Iowa State University

Homoscleromorpha is a small group in the phylum Porifera (Sponges) characterized by several morphological features (basement membrane, acrosomes in spermatozoa, and cross-striated rootlets of the flagellar basal apparatus) shared with eumetazoan animals but not found in most other sponges. To clarify the phylogenetic position of this group, we determined and analyzed the complete mitochondrial DNA (mtDNA) sequence of the homoscleromorph sponge *Oscarella carmela* (Porifera, Demospongiae). *O. carmela* mtDNA is 20,327 bp and contains the largest complement of genes reported for animal mtDNA, including a putative gene for the C subunit of the twin-arginine translocase (*tatC*) that has never been found in animal mtDNA. The genes in *O. carmela* mtDNA are arranged in 2 clusters with opposite transcriptional orientations, a gene arrangement reminiscent of those in several cnidarian mtDNAs but unlike those reported in sponges. At the same time, phylogenetic analyses based on concatenated amino acid sequences from 12 mitochondrial (mt) protein genes strongly support the phylogenetic affinity between the Homoscleromorpha and other demosponges. Altogether, our data suggest that homoscleromorphs are demosponges that have retained ancestral features in both mt genome and morphological organization lost in other taxa and that the most recent common ancestor of sponges and other animals was morphologically and genetically more complex than previously thought.

Introduction

Sponges (phylum Porifera) are an exclusively aquatic and predominantly filter-feeding group of animals consisting of approximately 15,000 extant species in 3 distinct groups; the Hexactinellida (glass sponges), the Calcarea (calcareous sponges), and the Demospongiae (demosponges) (Hooper and Van Soest 2002). Morphologically, sponges are built around an aquiferous system of canals and chambers, connected to the surrounding environment by multiple pores (hence the name Porifera). Histologically, the sponge body consists of 2 primary layers of cells (pinacoderm and choanoderm) and an inner cellular region (mesohyl) (Harrison and De Vos 1991). Pinacoderm, the outer layer of cells, lines the surface of the sponge and continues into internal canals where it is eventually replaced by the choanoderm, a layer of characteristic flagellated cells (choanocytes) surrounding the chambers. Choanocytes make up the principle "pump" and "filter" of the system, driving water through the sponge, trapping and phagocytizing suspended bacteria and other particulate food (De Vos et al. 1991). It is generally accepted that neither pinacoderm nor choanoderm constitutes the true epithelium (Woollacott and Pinto 1995; Tyler 2003). In fact, it is habitually stated that sponges do not possess any true tissues and thus represent an early stage in the evolution of animal multicellularity (Brusca RC and Brusca GJ 2002). Consequently, sponges have been often placed in the subkingdom Parazoa, separate from the true animals—Eumetazoa.

One group of sponges that challenges the view on Porifera as an ancestral animal phylum that never reached the tissue grade of organization is the subclass Homoscleromorpha. This small group (containing only 7 genera and about 60 species) is characterized by several unusual features, including unique cinctoblastula larvae that form by a unique process of multipolar egression, a basement membrane underlying both choanoderm and pinacoderm, flagellated pinacocytes, and distinctive morphology of aquiferous system and spicules (when present) (Gaino et al. 1987; Boute et al. 1996; Ereskovsky et al. 2002; Muricy and Diaz 2002). Recently, it has been shown that the basement membrane previously observed in adult homoscleromorphs is also lining the epithelial cells in homoscleromorph larvae and that these cells meet all criteria of true epithelia in higher animals: cell polarization, apical cell junctions, and a basement membrane (Boury-Esnault et al. 2003). Thus, at least one group of sponges has clearly reached the tissue grade of organization in its evolution. Interestingly, in addition to true epithelia, homoscleromorphs also share with "higher" animals the presence of acrosomes in spermatozoa (Baccetti et al. 1986; Boury-Esnault and Jamieson 1999) and (together with calcareous sponges) the presence of cross-striated rootlets in the flagellar basal apparatus of larval cells (Boury-Esnault et al. 2003; Maldonado 2004).

Three explanations are possible for these intriguing findings:

1. true epithelium, acrosomes, and cross-striated rootlets evolved independently in Homoscleromorpha and Eumetazoa;
2. these shared characters evolved in the common ancestor of sponges and other animals but were lost in most sponges;
3. Demosponges are not monophyletic; Homoscleromorpha shares a more recent common ancestor with Eumetazoa.

The choice among these alternative explanations has important implications for our understanding of the evolution of sponges and animals in general but requires knowledge of the phylogenetic position of the Homoscleromorpha. The latter, however, remains controversial.

Because of their distinct morphology and relatively simple anatomical organization, Homoscleromorpha has been traditionally regarded as one of the most primitive

Key words: Porifera, Homoscleromorpha, mtDNA, mitochondrial evolution, *tatC*.

E-mail: dlavrov@iastate.edu.

Mol. Biol. Evol. 24(2):363–373. 2007
doi:10.1093/molbev/msl167
Advance Access publication November 7, 2006

groups of demosponges (Lévi 1957), although a relationship to calcareous (calcaronean) sponges has also been proposed (Van Soest 1984; Grothe 1989; Grothe and Reitner 1990). Recent studies utilizing small subunit (SSU) and large subunit (LSU) ribosomal RNA (rRNA) sequences found no support for the inclusion of homoscleromorphs in the Demospongiae (Borchiellini et al. 2004; Nichols 2005), whereas the sister group relationship with Calcarea received some support from the Bayesian analysis of LSU ribosomal DNA (rDNA) data (Nichols 2005). The author of the latter study, however, downplays the significance of this association and points to the need of independent loci for the analysis of sponge relationships. Here, we describe the complete mitochondrial DNA (mtDNA) sequence from the homoscleromorph *Oscarella carmela* and analyze it in an attempt to clarify the phylogenetic position of this group.

Animal mtDNA is typically a small (~16 kb) circular-mapping molecule that contains 37 genes coding for 13 proteins, 2 rRNAs, and 22 transfer RNAs (tRNAs) (Boore 1999). These genes are usually compactly arrayed, have no introns, and their order is often stable over long evolutionary time. The mtDNAs of bilaterian animals are further distinguished by multiple deviations in the genetic code, unusual and/or reduced rRNA and tRNA primary and secondary structures, and the presence of a single large noncoding region (reviewed in Wolstenholme 1992). Demosponge mtDNA resemble that of most other animals in their compact organization, lack of introns, and a well-conserved gene order but at the same time contain several extra genes, encode bacterial-like rRNAs and tRNAs, and use a minimally derived genetic code in protein synthesis (Lavrov et al. 2005). Mitochondrial (mt) genomic data provide an excellent data set to investigate homoscleromorph relationships. In addition to the large amount of sequence data, which minimize the sampling error in sequence-based phylogenetic analysis, mtDNA harbors additional rare genomic characters useful for phylogenetic inference, including indels in the coding sequences, variations in the genetic code, changes in secondary structures of encoded tRNA and rRNAs, and gene rearrangements. The use of mt data is especially advantageous for the reconstruction of demosponge relationships because mt sequences evolve relatively slowly in this group, whereas the rate of gene rearrangements is relatively high (Lavrov and Lang 2005a; Lavrov et al. 2005).

Materials and Methods

Specimen Collection, DNA Extraction, mtDNA Amplification, Cloning, and Sequencing

A specimen of *O. carmela* (Class Demospongiae, Subclass Homoscleromorpha, Order Homosclerophorida, Family Plakinidae) (Muricy and Pearse 2004) was a gift from Scott A. Nichols (University of California, Berkeley). Total DNA was extracted from about 0.2 g of tissue fixed in 95% ethanol with a phenol–chloroform method modified from Saghai-Maroof (1984). Regions of mt *cox2* and *nad5* were amplified and sequenced using degenerate primers designed in our laboratory, checked against the GenBank database to exclude the possibility of contamination, and used to design specific primers for these regions:

Os-cox2-f1: 5′-CATATATGGTTCCTACTTCAGATC-3′
Os-cox2-r1: 5′-TTAACACCTAAAGATGGTACTGC-3′
Os-nad5-f1: 5′-GCGATAAACGAAATATCTCGACC-3′
Os-nad5-r1: 5′-TAGACCTAGTTGAGCTGATTTCC-3′

Complete *O. carmela* mtDNA was amplified in 2 overlapping fragments (~6 and 15 kbp in size) using the TaKaRa LA–PCR kit under recommended conditions. Random clone libraries were constructed from the purified PCR products using the TOPO Shotgun Subcloning Kit (Invitrogen, Carlsbad, CA). Plasmid preparation and sequencing were done at the Iowa State University Office of Biotechnology DNA facility. In addition to mtDNA, the nuclear SSU rRNA gene was amplified by PCR using modified versions of the universal eukaryotic primers A and B (Medlin et al. 1988) and used to confirm the proper taxonomic identification of the sample.

Assembly, Gene Identification, and Sequence Analysis

Sequencing reads were assembled using the STADEN software package (Staden 1996). To assure the quality of the final sequence, we manually checked the final assembly for sequencing errors and made sure that all genomic regions have either sequencing reads in both directions or at least 3 different reads in the same direction. Problematic and underrepresented regions in the assembly were sequenced directly from PCR products by primer walking. The tRNA genes were identified by the tRNAscan-SE program (Lowe and Eddy 1997); rRNA and protein genes were identified by similarity searches in local databases using the FASTA program (Pearson 1994) and in GenBank at National Center for Biotechnology Information (NCBI) using Blast network service (Benson et al. 2003). The secondary structures of rRNA genes were manually folded by analogy to published rRNA structures and drawn with the RnaViz 2 program (De Rijk et al. 2003).

Phylogenetic Analysis

Concatenated alignment of 2,812 amino acids deduced from 12 protein genes was created with ClustalW 1.82 (Thompson et al. 1994) and SOAP (Löytynoja and Milinkovitch 2001) programs via a previously described procedure (Lavrov et al. 2005). We performed a maximum likelihood (ML) search for the best tree with the TreeFinder (May 2006) program (Jobb et al. 2004) using the mtREV model of amino acid substitutions and 4 gamma categories. Bayesian inferences (MB) were conducted with MrBayes 3.1.1 (Ronquist and Huelsenbeck 2003). We used the mtREV model of amino acid substitutions with gamma + invariant distributed rates and ran 4 Markov Chain Monte Carlo chains for 1,100,000 generations. Trees were sampled every 1,000th cycle after the first 100,000 burn-in cycles. Molecular distances were calculated with the Tree-Puzzle 5.2 program (Strimmer and von Haeseler 1996) and the same substitution model as for the Bayesian analysis. The distance tree topology was inferred with the WEIGHBOR program (Bruno et al. 2000). For the bootstrap analysis of the distance data, a data set of 1,000 replicates was

generated by the SEQBOOT program in the PHYLIP package (Felsenstein 2005) and the distances for each data set were calculated using the "puzzleboot script" by Mike Holder and Andrew Roger (http://hades.biochem.dal.ca/Rogerlab/Software/software.html) and the programs listed above. The consensus bootstrap tree was calculated by the CONSENSE program of PHYLIP.

Results

Genome Organization: The Largest Set of Genes in Animal mtDNA, Unusual Gene Order, and High Coding Density

The mt genome of *O carmela* is a circular-mapping molecule 20,327 bp in size, and contains 15 protein-coding genes, 2 rRNA genes, and 27 tRNA genes; the largest complement of genes found in animal mtDNAs (fig. 1). In addition to the 37 genes typical for bilaterian mtDNAs (Wolstenholme 1992), genes for subunit 9 of adenosine triphosphate synthase (*atp9*), twin-arginine translocase component C (*tatC*), 3 extra tRNAs [*trnI*(cau), *trnR*(ucu), *trnM*(cau)e], as well as 2 duplicated trnX(nnn) are present in *O. carmela* mtDNA. Although 4 of these genes [*atp9*, *trnI*(cau), *trnR*(ucu), *trnM*(cau)e] have been previously described in other demosponge mt genomes (Lavrov et al. 2005), this is the first report of *tatC* in animal mtDNA.

The genes in *O. carmela* mtDNA are arranged into 2 clusters with opposite transcriptional orientations that subdivide the genome into 2 nearly equal parts of 9,842 and 10,485 bp. The change in the transcriptional polarity occurs between *cox1* and *cox2* and between *trnM*(cau)*e* and *cob*, putative transcription initiation and termination sites, respectively (fig. 1). The arrangement of genes into 2 transcriptional units is unique among demosponge mtDNAs, where all genes are typically transcribed from the same mtDNA strand (Lavrov and Lang 2005a; Lavrov et al. 2005; Lavrov DV, Wang X, unpublished data) but has been found in several other animal groups. In particular, mtDNA from 2 cnidarians, the moon jelly *Aurelia aurita* (Shao et al. 2006) and the octocoral *Sarcophyton glaucum* (Beaton et al. 1998), have similar arrangements of genes with transcription polarity changing at the same gene junction between *cox1* and *cox2*. Aside from −*cox1*+*cox2* gene boundaries, several other mt gene arrangements are shared between *O. carmela* and other animals (fig. 2), indicating a moderate number of rearrangements in this genome.

The *O. carmela* mtDNA is a compact genome that contains only 1,275 noncoding bp (6.27% of the genome sequence). These noncoding nucleotides are distributed among 43 intergenic regions 1–130 bp in size. Twenty of the intergenic regions contain more than 20 bp, and 3, located between *nad2* and *nad5*, *trnF* and *cox3*, *cox1* and *cox2*, are larger than 100 bp. We found no significant similarity between any of these regions and the existing sequences in GenBank.

Nucleotide Composition and Codon Usage: Prevalence of Selection over Mutational Biases

The A + T content of *O. carmela* mtDNA is 66.4%, similar to those of other demosponge mt genomes. However, in contrast to the other genomes, the 2 strands of *O. carmela* mtDNA do not differ significantly in nucleotide composition (the total AT and GC skews are 0.02 and 0, respectively). This lack of strand asymmetry in *O. carmela* mtDNA is the result of opposite nucleotide biases in part I (*cox2-cob*) and part II (*cox1-M*) of this genome (coding strands in both parts have positive GC skews [0.13 and 0.12, respectively] and negative AT skews [−0.02 and −0.06, respectively], which cancel each other when the whole sequence is considered). Among different types of genes, protein genes and tRNA genes display negative AT skews, whereas rRNA genes show positive AT skews; all types of genes display positive GC skews (table 1). Among individual genes, only *atp8* deviates from the described pattern and has a negative GC skew and a positive AT skew (supplementary table S1, Supplementary Material online). Interestingly, in the case of protein-coding genes the GC skew is strongly positive (0.38) at the first-codon positions, negative (−0.17) at the second, and weakly positive (0.09) at the third. Similarly, AT skew is weakly negative (−0.02) at the first position, strongly negative (−0.37) at the second, but positive (0.06) at the third (table 1). Thus, selection for specific amino acids appears to play a dominant role in shaping the nucleotide skews between the 2 strands of *O. carmela* mtDNA. At the same time, proposed cytosine deamination in the process of asymmetrical replication and transcription (Francino et al. 1996; Lobry 1996; Francino and Ochman 1997; Frank and Lobry 1999) may also play some role in strand asymmetry as evident from the presence

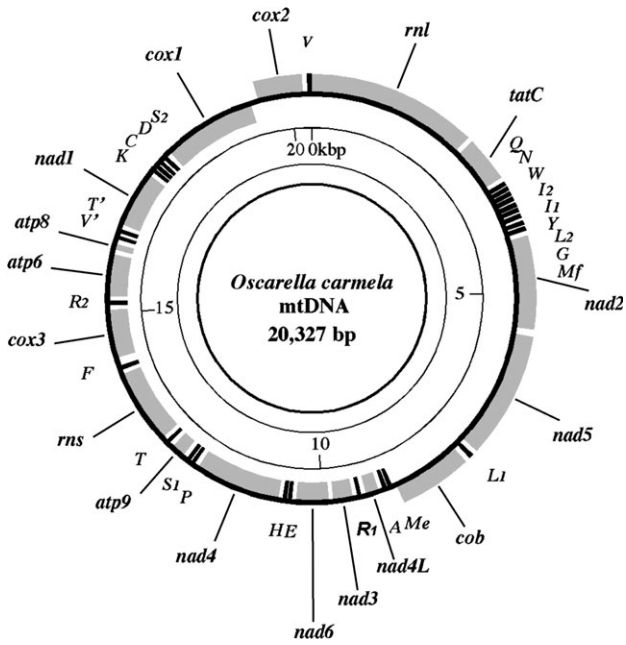

FIG. 1.—Genome map of *Oscarella carmela* mtDNA. Protein and ribosomal genes (gray) are *atp6*, *atp8–9*: subunits 6, 8, and 9 of F_0 adenosine triphosphatase (ATP) synthase; *cox1–3*: cytochrome c oxidase subunits 1–3; *cob*: apocytochrome b; *nad1–6* and *nad4L*: NADH dehydrogenase subunits 1–6 and 4L; *tatC*: twin-arginine translocase component C; *rns* and *rnl*: SSU and LSU rRNAs. The tRNA genes (black) are identified by the one-letter code for their corresponding amino acid; subscripts denote different genes for isoacceptor tRNAs; apostrophes (*T′* and *V′*) indicate duplicated tRNA genes. Genes are transcribed in two directions: clockwise (*cox2-cob*) and counterclockwise (*cox1-Me*).

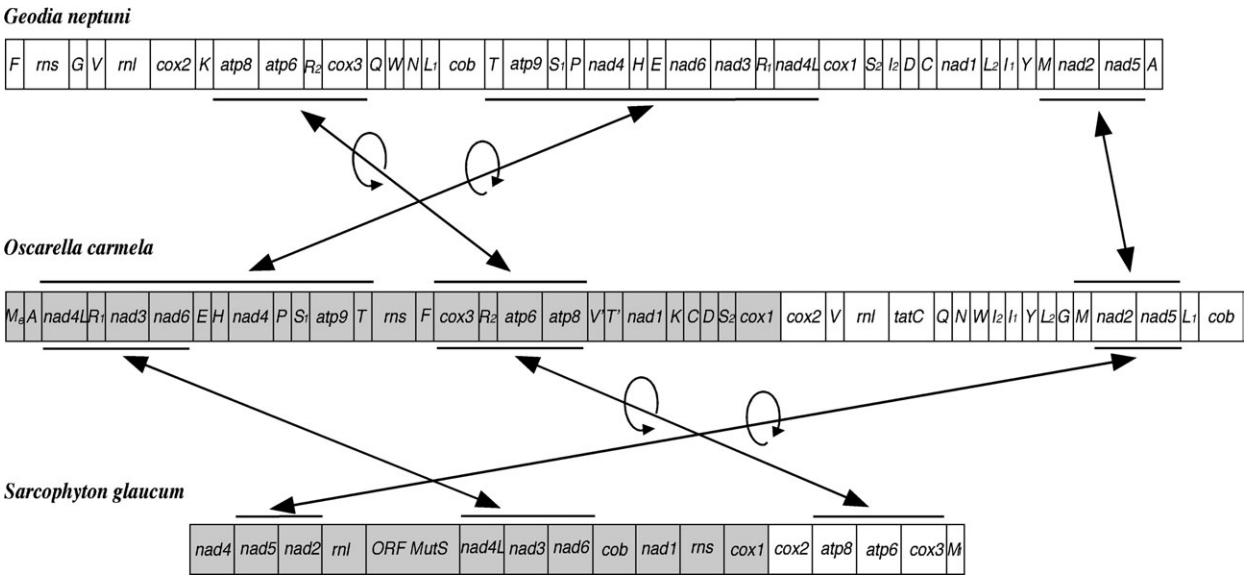

FIG. 2.—Comparison of gene arrangements in the mtDNAs of the homoscleromorph *Oscarella carmela*, demosponge *Geodia neptuni*, and cnidarian *Sarcophyton glaucum*. Genes are not drawn to scale; protein and rRNA genes are indicated by larger boxes and tRNA genes by smaller boxes. Open boxes indicate transcriptional direction from left to right, filled boxes from right to left. Conserved blocks of genes shared between different organisms are underlined and interconnected with arrows. All abbreviations and other symbols are as in figure 1.

of nucleotide skews at the third-codon position and in the intergenic regions (table 1).

Synonymous codon usage largely correlates with the nucleotide biases in the coding strand: codons ending with A or T are clearly preferred (80.9%), whereas those ending with C are the least frequent (table 2). Out of 62 codons expected to specify an amino acid, 1 (CGC) is not found in the mt protein genes of *O. carmela*, as well as other demosponges (Lavrov et al. 2005). No significant differences were found in the codon usage in protein genes encoded by part I and part II of the mtDNA.

Protein Genes: The First Report of *tatC* in Animal mtDNA

We identified 15 protein-coding genes in the *O. carmela* mt genome. Fourteen of them (*atp6*, *atp8–9*, *cob*, *cox1–3*, *nad1–6*, *nad4L*) have been previously reported in demosponge mtDNAs (Lavrov et al. 2005). These genes, coding for protein subunits involved in respiration and oxidative phosphorylation, are similar in sizes to their homologues in other demosponges mtDNAs (±7%, except for *atp8* which is 21% smaller than that in *Tethya actinia* mtDNA) and share with them on average 69.8% (27.2–89.3%) of inferred amino acid identity (table 3). As expected, more variation in size and lower sequence identity were found in comparisons of *O. carmela* mt protein–coding genes with their homologues in *Metridium senile* (table 3) and other animals (not shown).

In addition to the protein genes described above, an open reading frame (ORF) has been found in the *O. carmela* mt sequence and identified as *tatC* based on sequence similarity searches, presence of conserved domains, and predicted secondary structure (fig. 3, see below). The *tatC* (also known as *ymf16* and *mttB*) codes for the largest and usually the most conserved subunit of the twin-arginine transport (Tat) pathway (Bogsch et al. 1998), which exists in prokaryotic organisms, chloroplasts, and some mitochondria, and functions in the transport of fully folded proteins and enzyme complexes across membranes (for a comprehensive review, see Berks et al. 2003). Previously,

Table 1
Nucleotide Composition of *Oscarella carmela* mtDNA

	Coding Sequences								
	Codon Position								
	First	Second	Third	Total	rRNA Genes	tRNA Genes	Intergenic	Part I (*cox2-cob*) Total	Part II (*cox1-trnM*) Total
%G	26.8	15.1	10.4	17.5	22.2	23.8	15.8	19.0	18.8
%A	29.9	20.2	42.9	31.0	35.4	27.0	33.9	32.5	31.2
%T	31.3	43.5	37.9	37.6	26.8	31.1	35.1	33.9	35.2
%C	11.9	21.1	8.7	13.9	15.6	18.0	15.1	14.6	14.8
%(A + T)	61.2	63.7	80.9	68.6	62.2	58.2	69.1	66.4	66.4
AT skew	−0.02	−0.37	0.06	−0.10	0.14	−0.07	−0.02	−0.02	−0.06
GC skew	0.38	−0.17	0.09	0.11	0.18	0.14	0.03	0.13	0.12
Total (bp)	4,420	4,420	4,420	13,260	3,801	1,991	1,275	9,842	10,485

Table 2
Codon Usage among the 14 Genes Coding for Protein Subunits Involved in Respiration and Oxidative Phosphorylation and, Separately, *tatC*

		Aa	*tatC*			Aa	*tatC*			Aa	*tatC*			Aa	*tatC*
Phe	TTT	269	20	Ser	TCT	98	8	Tyr	TAT	159	16	Cys	TGT	31	6
	TTC	45	0		TCC	11	2		TAC	25	3		TGC	6	0
Leu	TTA	404	26		TCA	88	1	Ter	TAA	12	1	Trp	TGA	76	4
	TTG	38	6		TCG	10	1		TAG	2	0		TGG	14	1
Leu	CTT	72	1	Pro	CCT	56	4	His	CAT	59	3	Arg	CGT	8	2
	CTC	10	0		CCC	19	3		CAC	21	0		CGC	0	0
	CTA	63	2		CCA	71	2	Gln	CAA	78	4		CGA	23	0
	CTG	8	1		CCG	6	0		CAG	8	1		CGG	3	0
Ile	ATT	156	18	Thr	ACT	87	6	Asn	AAT	97	8	Ser	AGT	68	5
	ATC	38	2		ACC	17	2		AAC	28	1		AGC	24	2
	ATA	272	27		ACA	118	1	Lys	AAA	102	8	Arg	AGA	50	6
Met	ATG	132	5		ACG	11	1		AAG	13	3		AGG	13	1
Val	GTT	118	5	Ala	GCT	119	3	Asp	GAT	74	4	Gly	GGT	93	2
	GTC	11	0		GCC	52	1		GAC	29	0		GGC	33	1
	GTA	129	3		GCA	109	0	Glu	GAA	94	8		GGA	110	5
	GTG	43	0		GCG	26	1		GAG	30	2		GGG	78	3

NOTE.—Aa, amino acid.

tatC has been reported in mtDNA of plants and protists (including closely related to animals choanoflagellate *Monosiga brevicolis*) but has never been found in either animal or fungal mtDNA (Yen et al. 2002; note that *Thraustochytrium aurelum* identified as "marine fungus" in the cited paper is actually a stramenopile alga).

The inferred size of *tatC* in *O. carmela* is 759 bp, typical for homologous genes in other organisms (Yen et al. 2002). This size estimate is based on our assignment of TTG as the initiation codon for *tatC* (the closest in-frame ATG codon is 252 nt downstream). Although this start codon is unusual, it has been reported as an initiation codon in other organisms (Golderer et al. 1995; Ko and Smith 1999; Baar et al. 2003) as well as in mt protein–coding genes (Okimoto et al. 1990) and may be used to regulate the expression of the *tatC* relative to other mitochondrially encoded genes (Okimoto et al. 1990; Golderer et al. 1995). The derived amino acid sequence of *O. carmela* TatC is 27% and 19% identical with those of *Reclinomonas americana* and *M. brevicollis*, respectively.

Blast searches against the raw sequences from the nuclear genome of the demosponge *Amphimedon queenslandica* (Hooper and Van Soest 2006) and the complete nuclear genomes of other animals identified a *tatC*-like sequence only in the demosponge genome (NCBI trace archive database; reads 922482408, 922482312; 25% of inferred amino acid identity). This finding suggests that the fate of this gene may have been different in sponges than in other animals (transfer to the nucleus vs. loss). Alternatively, it is possible that the gene still exists in the nuclear genomes of other animals but has evolved beyond recognition.

Table 3
Comparison of mt Protein Genes in *Oscarella carmela* (OC) with Those of demosponges *Geodia neptuni* (GN) and *Tethya actinia* (TA), cnidarian *Metridium senile* (MS), and Choanoflagellate *Monosiga brevicollis* (MB)

	Number of Encoded Amino Acids[a]		% Amino Acid Identity							Predicted Initiation and Termination Codons in OC	
Gene	OC	GN	TA	MS	MB	OC/GN	OC/TA	OC/MS	OC/MB	Initiation Codons	Stop Codons
atp6	245	244	244	229	252	65.7	69.4	64.1	51.6	ATG	TAA
atp8	66	63	80	72	99	37.9	27.2	39.4	17.2	ATG	TAA
atp9	76	78	78	—	73	83.3	78.2	—	69.2	ATG	TAA
cob	400	381	381	393	380	67.8	67.0	65.4	62.2	ATG	TAA
cox1	521	520	522	530	534	84.8	89.3	85.1	70.9	ATG	TAA
cox2	249	247	243	248	256	78.7	77.9	76.6	54.8	ATG	TAG
cox3	261	262	262	262	263	78.6	78.6	79.0	60.8	ATG	TAA
nad1	328	327	338	334	343	72.5	76.9	71.8	62.4	ATG	TAA
nad2	465	465	481	385	546	62.4	58.3	53.9	34.3	ATG	TAA
nad3	118	118	118	118	118	67.8	72.9	72.9	62.7	ATG	TAA
nad4	495	481	482	491	498	67.9	70.3	69.1	57.7	ATG	TAG
nad4L	99	106	99	99	99	68.9	83.8	74.7	60.6	ATG	TAA
nad5	633	603	622	600	688	71.1	74.4	69	51.9	ATG	TAA
nad6	197	185	187	202	228	62.3	61.6	51.4	37.3	GTG	TAA
tatC	253	—	—	—	234	—	—	—	18.7	TTG	TAA

[a] Data for *G. neptuni* and *T. actinia* are from Lavrov et al. (2005); for *M. senile* from Beagley et al. (1998); and for *M. brevicolis* from Burger et al. (2003).

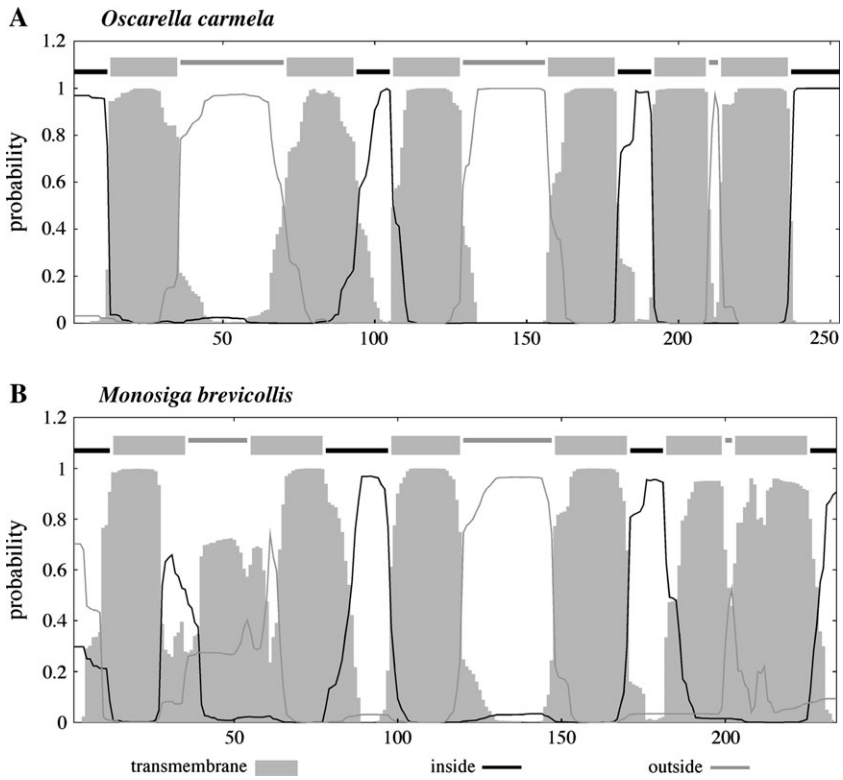

FIG. 3.—Predicted secondary structures of mitochondrially encoded TatC protein in *Oscarella carmela* (*A*) and *Monosiga brevicollis* (*B*). The secondary structure and transmembrane regions were analyzed on the TMHMM server v. 2.0 (Krogh et al. 2001; Sonnhammer et al. 1998). The *x* axis designates amino acid positions in each protein. The *y* axis shows posterior probabilities for each prediction.

rRNA Genes (*rns*, *rnl*) Encode Well-conserved rRNA Molecules

Genes for the SSU and LSU rRNAs (*rns* and *rnl*, respectively) have been found in *O. carmela* mtDNA and the secondary structures of encoded rRNAs have been modeled by analogy with homologous molecules (supplementary figs. S1 and S2, Supplementary Material online). The *rns* and *rnl* are located more than 5 kbp apart in the genome and have opposite transcriptional polarities (fig. 1). Such arrangement is unusual for demosponge mtDNA where *rns* and *rnl* are usually separated by 2 tRNA genes (*rns-trnG-trnV-rnl*) (Lavrov et al. 2005; Lavrov DV, Wang X, unpublished data) and relatively rare in animal mtDNA in general. Based on secondary structure modeling, we deduced the length of *rns* as 1,281 bp (making it the largest mt-*rns* described for animals) and the length of *rnl* as 2,520 bp (similar to homologous genes in other demosponges). The larger size of *O. carmela rns* is mostly due to the better conservation of stem 39, which has a similar size in *O. carmela* and *Escherichia coli* but is reduced in other demosponges (supplementary fig. S1, Supplementary Material online). The loop at the end of stem 33 also has a 15-nt insertion in the *O. carmela* mt SSU RNA. In contrast, only small indels (less than 10 nt) were found in *O. carmela rnl*. These include insertions in stem 54 and loops adjacent to stems 25, 52, and 101. The primary sequence of *O. carmela rns* and *rnl* are well conserved and share on average 65.8% and 68.1% of sequence identity with homologous genes in *Geodia neptuni* and *T. actinia*, 43.2% and 50.6% of sequence identity with their homologues in the choanoflagellate *M. brevicolis*, and 44.1% and 47.7% of sequence identity with those in *E. coli*, respectively.

Duplicated tRNA Genes, Canonical tRNA Structures, and Unusual *trnP(ugg)*

Twenty-seven tRNA genes have been identified in *O. carmela* mtDNA, and their inferred secondary structures are shown in supplementary figure S3 (Supplementary Material online). These genes include the same set of 24 tRNA genes found in 3 other demosponges (Lavrov and Lang 2005b), an additional gene for an elongator $tRNA^{Met}_{CAU}$ previously reported only in *T. actinia* among demosponges (Lavrov et al. 2005), and duplicated genes for $tRNA^{Val}_{UAC}$ and $tRNA^{Thr}_{UGU}$. The 2 copies of $tRNA^{Thr}_{UGU}$ have only 1-nt difference and are located about 5 kb away in the same transcription strand (part II, *cox1-M*), whereas those of $tRNA^{Val}_{UAC}$ have a 4-nt difference and are located in different transcriptional strands. The duplicated copies of genes for $tRNA^{Thr}_{UGU}$ (*T′*) and $tRNA^{Val}_{UAC}$ (*V′*) are adjacent in *O. carmela* mtDNA (fig. 1). The duplication mechanism for these genes is unknown but is unlikely to be due to the commonly invoked duplication–random loss model (Boore 2000) because it would explain neither the clustering of the duplicated genes in the same region of the genome nor the change in the transcriptional polarity of *trnV*(uac).

The primary sequences of *O. carmela* tRNA genes share 55.4–91.7% (average = 73.8%) sequence identity with homologous genes in *G. neptuni* and *T. actinia*.

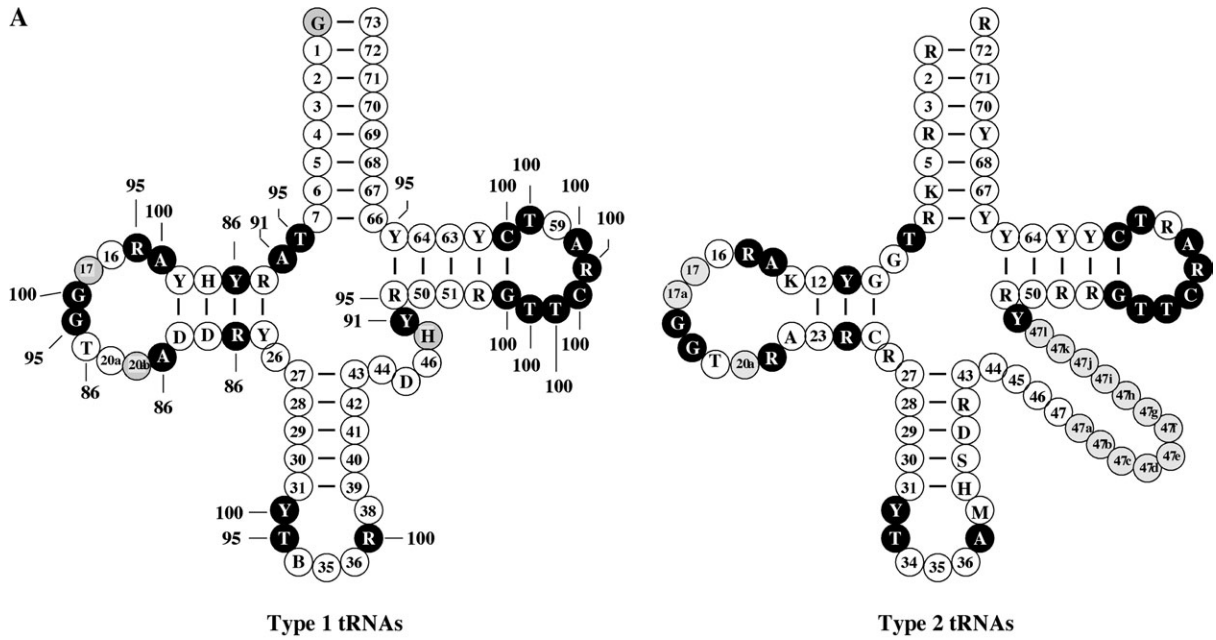

B

Porifera/Placozoa	11 - 24 pair	Bilateria/Outgroups	11 - 24 pair
Oscarella carmela	A - T	*Amoebidium parasiticum*	C - G
Geodia neptuni	A - T	*Monosiga brevicollis*	T - A
Tethya actinia	A - T	*Drosophila yakuba*	T - A
Axinella corrugata	A - T	*Homo sapiens*	T - A
Trichoplax adhaerens	A - T		

FIG. 4.—Consensus secondary structures for *Oscarella carmela* type 1 (with short variable arm) and type 2 (with long variable arm) mt-tRNAs (*A*) and comparison of 11–24 bp in tRNA proline (*B*). Numbering of nucleotides is based on the convention used for yeast tRNA phenylalanine (Robertus et al. 1974). Open circles with numbers: nucleotides are present in all tRNAs; open circles with letters: nucleotide combinations present in all tRNAs; filled black circle: nucleotides or nucleotide combinations that are described as invariant or semi-invariant in prokaryotic and eukaryotic nuclear-encoded tRNAs with frequencies (percentages) for *O. carmela* type1 mt-tRNAs shown by accompanying numbers (all these nucleotides are 100% conserved in type 2 tRNAs); and filled gray circles: nucleotides present in some but not all tRNAs.

The most conserved tRNA is $tRNA^{Try}_{UCA}$ (the average identity with the 2 demosponges is 84.5%) and the least conserved is $tRNA^{Glu}_{UUG}$ (the average identity is 59.6%). The consensus primary sequences and secondary structures for type 1 (with short variable arm) and type 2 (with long variable arm) *O. carmela* mt-tRNAs are shown in figure 4. As can be seen from this figure, most nucleotides involved in tRNA tertiary interactions (including G18–U55 and G19–C56 interactions between D- and T-loops) are well conserved in *O. carmela* mt-tRNAs.

Interestingly, we found a highly unusual A11–T24 pair in *O. carmela* $tRNA^{Pro}_{UGG}$, similar to the animal-specific R11–Y24 pair in $tRNA^{Trp}_{UCA}$ (Wolstenholme 1992; Lavrov et al. 2005). The A11–T24 pair is also present in mt-*trnP(ugg)* genes from other demosponges (Lavrov and Lang 2005b) as well as the placozoan *Trichoplax adhaerens* (Dellaporta et al. 2006) but is not found in homologous genes of either the outgroups *M. brevicolis* and *Amoebidium parasiticum* or the bilaterian animals (fig. 4B). Because the R11–Y24 bp is an important recognition element for initiator tRNA, it is usually strongly counterselected in elongator tRNAs (Marck and Grosjean 2002), and its presence in $tRNA^{Pro}_{UGG}$ of demosponges and *T. adhaerens* may be phylogenetically significant (see below).

Sequence-based Phylogenetic Analysis Supports the Demosponge Affinity of the Homoscleromorpha

Phylogenetic analysis based on the concatenated amino acid sequences inferred from 12 mt protein genes recovers an overall conventional tree of eukaryotic relationships but with "lower" animals (phyla Porifera, Cnidaria, and Placozoa) forming a monophyletic group (fig. 5). This clustering of non-bilaterian animals has been previously explained by elevated rates of mt evolution in Bilateria, which would pull the latter group toward the base of metazoan tree (Lavrov et al. 2005). However, the presence of a highly unusual A11–T24 pair in mt – $tRNA^{Pro}_{UGG}$ of demosponges and *T. adhaerens* (cnidarians do not encode this tRNA in mtDNA) provides an additional character supporting this

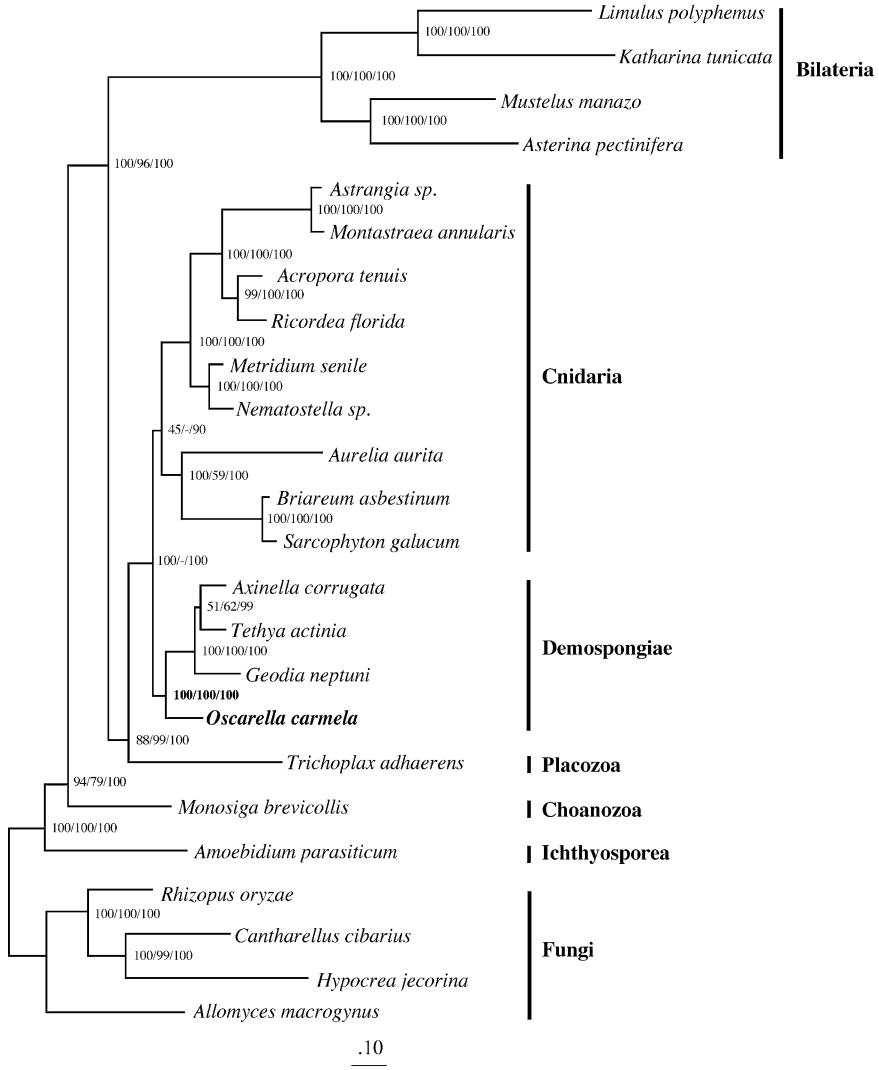

FIG. 5.—Phylogenetic position of the homoscleromorph *Oscarella carmela* based on maximum likelihood (ML), Bayesian (MB), and weighted neighbor joining (WNJ) analyses of concatenated amino acid sequences inferred from 12 protein genes. The first number at each node indicates the percentage of bootstrap support in ML analysis; the second numberdenotes the percentage of bootstrap support in WNJ analysis; and the third number shows the posterior probability in MB analysis. The protein sequences for *Cantharellus cibarius*, *Hypocrea jecorina*, and *Rhizopus oryzae* were downloaded from http://megasun.bch.umontreal.ca/People/lang/FMGP/proteins.html. Other protein sequences were derived from the GenBank files: *Katharina tunicata* U09810, *Limulus polyphemus* AF216203, *Asterina pectinifera* D16387, *Mustelus manazo* AF347015, *Acropora tenuis* AF338425, *Astrangia* sp. DQ643832, *Briareum asbestinum* DQ640649, *Metridium senile* AF000023, *Montastraea annularis* AP008974, *Nematostella* sp. DQ643835, *Ricordea florida* DQ640648, *Sarcophyton glaucum* AF064823 and AF063191, *Aurelia aurita* DQ787873, *Geodia neptuni* AY320032, *Tethya actinia* AY320033, *Axinella corrugata* AY791693, *Trichoplax adhaerens* DQ112541, *Amoebidium parasiticum* AF538042–AF538052, *Monosiga brevicollis* AF538053, and *Allomyces macrogynus* U41288.

clade. Thus, further studies are clearly needed to investigate these contentious relationships.

Within Metazoa, *O. carmela* groups with other demosponges with 100% support in ML, Weighted Neighbor-Joining (WNJ), and Bayesian analyses (fig. 5). Furthermore, this relationship received 98% bootstrap support in MP analysis using original data and 94% bootstrap support in MP analysis where individual amino acids were recoded into the 6 Dayhoff categories as in Embley et al. (2003). The results of our analyses are robust with respect to taxa selection and do not change when preliminary sequences from several mt genes from glass and calcareous sponges are included in the data set or when bilaterian taxa are removed from the analysis (not shown). The sister group relationship between *O. carmela* and other demosponges is also recovered by the ML analysis for 8 out of 12 individual mt protein genes (*atp6*, *cob*, *cox2*, *cox3*, *nad1*, *nad2*, *nad4*, and *nad5*). The analyses of the remaining genes produced 4 different placements for *O. carmela* (supplementary fig. S4, Supplementary Material online).

Discussion and Conclusion

Our analysis of *O. carmela* mtDNA revealed several genomic features potentially informative for understanding the phylogenetic position of the Homoscleromorpha. Here we discuss these features with respect to 3 possible phylogenetic hypotheses: 1) Homoscleromorpha diverged from

the animal lineage prior to other demosponges; 2) Homoscleromorpha is more closely related to demosponges than to Eumetazoa; and 3) Homoscleromorpha is more closely related to Eumetazoa than to demosponges. It should be noted that because of the scarcity of data from glass and calcareous sponges, we could not test the monophyly of the Demospongiae in the present study.

The first of these hypotheses is supported by the presence of an extra protein gene (*tatC*) in *O. carmela* mtDNA. Because this gene is mitochondrially encoded in multiple outgroups, including the choanoflagellate *M. brevicolis*, but is absent in other animal mtDNA, the most parsimonious reconstruction is a single loss of *tatC* after the divergence between the Homoscleromorpha and other animals. Unfortunately, it is well known that the lack of mt genes is not a reliable phylogenetic character, and that parallel independent losses from organellar DNA are common (Martin et al. 1998). Our finding of a *tatC*-like sequence in the nuclear genome of *A. queenslandica* but not other animals hints to such independent events in *tatC* evolution and suggests that the fate of this gene was different in demosponges and bilaterian animals (transfer to the nucleus vs. loss). The only other feature supporting the basal position of the Homoscleromorpha is the conservation of some helices in *O. carmela* mt SSU RNA secondary structure—not a strong phylogenetic character either. Overall, we regard the support for the first hypothesis as weak.

The second hypothesis, the inclusion of Homoscleromorpha within the monophyletic Demospongiae and/or Porifera, is supported by the phylogenetic analysis of the mt sequence data. The grouping of *O. carmela* with other demosponges is robust with respect to different selections of genes, taxa, models, and phylogenetic methods. Furthermore, we searched for, but could not identify, any potential biases in either nucleotide composition or rates of sequence evolution that would cause this association. Therefore, we posit that our results reflect a genuine phylogenetic signal present in the mt data set rather than an artifact of phylogenetic reconstruction.

Finally, our data provide no support for the closer phylogenetic relationship of the Homoscleromorpha to the Eumetazoa rather than the Demospongiae. It may appear that similar mt gene arrangements in *O. carmela* and several cnidarians support this phylogenetic hypothesis, but this is not the case. The reported similarities can be equally parsimoniously explained by these arrangements being plesiomorphic for all animals (or for nonbilaterian animals if the latter group is indeed monophyletic). Unfortunately, we are not able to distinguish between these possibilities due to the lack of informative outgroups outside the Metazoa.

If Homoscleromorpha forms a monophyletic group with demosponges (and potentially other sponges), then the finding of morphological features shared between this group and Eumetazoa (acrosomes in spermatozoa, true epithelia with basal lamina, and cross-striated rootlets) is most easily explained by the presence of these features in the common ancestor of sponges and other animals and their subsequent loss in most (but not all) sponge lineages. (Some of the morphological features discussed above have been reported in other demosponges: a network of collagen fibers underlining larval ciliated cells has been described in *Crambe crambe* [Maldonado 2004], the sperms with acrosomes have been found in *C. crambe* and *Crellomima imparidens* [Ereskovsky 2005], and striated rootlets of the basal body have been found in *Mycal contarenii* larva [Lévi 1964].) If this is indeed the case, then the common ancestor of sponges and other animals should have been morphologically more complex than modern sponges, which may represent an adaptive simplification to their sessile and filter-feeding life style. An alternative explanation would need to involve an independent origin of similar morphological characters in several animal lineages, an unlikely scenario in our view. Interestingly, a similar deduction has been made recently by Maldonado (2004), based on an independent reassessment of embryological and histological data from sponges.

Supplementary Material

Amino acid alignment used in phylogenetic analyses, supplementary table S1, and supplementary figure S1–S4 are available at *Molecular Biology and Evolution* online (http://www.mbe.oxfordjournals.org/). *Oscarella carmela* mt genome sequence has been deposited in the GenBank database under the accession number EF081250.

Acknowledgments

We thank Scott Nichols for the samples of *O. carmela*; Alexander Ereskovsky, Karri Haen, Sally Leys, and Scott Nichols for valuable comments on an earlier version of the manuscript; and the College of Liberal Arts and Sciences at Iowa State University for funding.

Literature Cited

Baar C, Eppinger M, Raddatz G, et al. (15 authors). 2003. Complete genome sequence and analysis of *Wolinella succinogenes*. Proc Natl Acad Sci USA. 100:11690–11695.

Baccetti B, Gaino E, Sara M. 1986. A sponge with acrosome: *Oscarella lobularis*. J Ultrastruct Mol Struct Res. 94: 195–198.

Beagley CT, Okimoto R, Wolstenholme DR. 1998. The mitochondrial genome of the sea anemone *Metridium senile* (Cnidaria): introns, a paucity of tRNA genes, and a near-standard genetic code. Genetics. 148:1091–1108.

Beaton MJ, Roger AJ, Cavalier-Smith T. 1998. Sequence analysis of the mitochondrial genome of *Sarcophyton glaucum*: conserved gene order among octocorals. J Mol Evol. 47:697–708.

Benson DA, Karsch-Mizrachi I, Lipman DJ, Ostell J, Wheeler DL. 2003. GenBank. Nucleic Acids Res. 31:23–27.

Berks BC, Palmer T, Sargent F. 2003. The Tat protein translocation pathway and its role in microbial physiology. Adv Microb Physiol. 47:187–254.

Bogsch EG, Sargent F, Stanley NR, Berks BC, Robinson C, Palmer T. 1998. An essential component of a novel bacterial protein export system with homologues in plastids and mitochondria. J Biol Chem. 273:18003–18006.

Boore JL. 1999. Animal mitochondrial genomes. Nucleic Acids Res. 27:1767–1780.

Boore JL. 2000. The duplication/random loss model for gene rearrangement exemplified by mitochondrial genomes of deuterostome animals. In: Sankoff D, Nadeau JH, editors. Comparative genomics. Dordrecht: Kluwer Academic Publishers. p. 133–147.

Borchiellini C, Chombard C, Manuel M, Alivon E, Vacelet J, Boury-Esnault N. 2004. Molecular phylogeny of Demospongiae: implications for classification and scenarios of character evolution. Mol Phylogenet Evol. 32:823–837.

Boury-Esnault N, Ereskovsky A, Bezac C, Tokina D. 2003. Larval development in the Homoscleromorpha (Porifera, Demospongiae). Invertebr Biol. 122:187–202.

Boury-Esnault N, Jamieson BGM. 1999. Porifera. In: Jamieson BGM, editor. Progress in male gamete ultrastructure and phylogeny. Chichester (NY): John Wiley & sons. p. 1–20.

Boute N, Exposito JY, Boury-Esnault N, Vacelet J, Noro N, Miyazaki K, Yoshizato K, Garrone R. 1996. Type IV collagen in sponges, the missing link in basement membrane ubiquity. Biol Cell. 88:37–44.

Bruno WJ, Socci ND, Halpern AL. 2000. Weighted neighbor joining: a likelihood-based approach to distance-based phylogeny reconstruction. Mol Biol Evol. 17:189–197.

Brusca RC, Brusca GJ. 2002. Invertebrates. Sunderland (MA): Sinauer Associates.

Burger G, Forget L, Zhu Y, Gray MW, Lang BF. 2003. Unique mitochondrial genome architecture in unicellular relatives of animals. Proc Natl Acad Sci USA. 100:892–897.

Dellaporta SL, Xu A, Sagasser S, Jakob W, Moreno MA, Buss LW, Schierwater B. 2006. Mitochondrial genome of *Trichoplax adhaerens* supports placozoa as the basal lower metazoan phylum. Proc Natl Acad Sci USA. 103:8751–8756.

De Rijk P, Wuyts J, De Wachter R. 2003. RnaViz 2: an improved representation of RNA secondary structure. Bioinformatics. 19:299–300.

De Vos L, Rutzler K, Boury-Esnault JV, Donadey C, Vacelet J. 1991. Atlas of sponge morphology = Atlas de morphologie des éponges. Washington (DC): Smithsonian Institution Press.

Embley TM, van der Giezen M, Horner DS, Dyal PL, Foster P. 2003. Mitochondria and hydrogenosomes are two forms of the same fundamental organelle. Philos Trans R Soc Lond B Biol Sci. 358:191–201 [discussion 201–202].

Ereskovsky AV. 2005. Comparative embryology of sponges. St. Petersburg (Russia): St. Petersburg State Univ Press.

Ereskovsky AV, Boury-Esnault N. 2002. Cleavage pattern in Oscarella species (Porifera, Demospongiae, Homoscleromorpha): transmission of maternal cells and symbiotic bacteria. J Nat Hist. 36:1761–1775.

Felsenstein J. 2005. PHYLIP (phylogeny inference package). Version 3.65. Distributed by the author. Seattle (WA): Department of Genome Sciences, University of Washington.

Francino MP, Chao L, Riley MA, Ochman H. 1996. Asymmetries generated by transcription-coupled repair in enterobacterial genes. Science. 272:107–109.

Francino MP, Ochman H. 1997. Strand asymmetries in DNA evolution. Trends Genet. 13:240–245.

Frank AC, Lobry JR. 1999. Asymmetric substitution patterns: a review of possible underlying mutational or selective mechanisms. Gene. 238:65–77.

Gaino E, Burlando B, Buffa P. 1987. Structural and ultrastructural aspects of growth in *Oscarella lobularis* (Porifera, Demospongiae). Growth. 51:451–460.

Golderer G, Dlaska M, Grobner P, Piendl W. 1995. TTG serves as an initiation codon for the ribosomal protein MvaS7 from the archaeon *Methanococcus vannielii*. J Bacteriol. 177:5994–5996.

Grothe F. 1989. On the phylogeny of homoscleromorphs. Berl Geowiss Abh Reiche A Geolog Palaeont. 106:155–164.

Grothe F, Reitner J. 1990. Discussion on the phylogenetic position of the Homoscleromorpha (Porifera). Berl Geowiss Abh Reiche A Geolog Palaeont. 100:16–17.

Harrison FW, De Vos L. 1991. Porifera. In: Harrison FW, Westfall JA, editors. Microscopic anatomy of invertebrates. Vol. 2. Placozoa, Porifera, Cnidaria, and Ctenophora. New York: Wiley-Liss. p. 29–89.

Hooper JNA, Van Soest RWM. 2002. Class Demospongiae Sollas, 1885. In: Hooper JNA, Van Soest RWM, editors. Systema Porifera: a guide to the classification of sponges. New York: Kluwer Academic/Plenum Publishers. p. 15–18.

Hooper JNA, Van Soest RWM. 2006. A new species of Amphimedon (Porifera, Demospongiae, Haplosclerida, Niphatidae) from the Capricorn-Bunker group of islands, Great Barrier Reef, Australia: target species for the 'sponge genome project'. Zootaxa. 1314:31–39.

Jobb G, von Haeseler A, Strimmer K. 2004. TREEFINDER: a powerful graphical analysis environment for molecular phylogenetics. BMC Evol Biol. 4:18.

Ko R, Smith LT. 1999. Identification of an ATP-driven, osmoregulated glycine betaine transport system in Listeria monocytogenes. Appl Environ Microbiol. 65:4040–4048.

Krogh A, Larsson B, von Heijne G, Sonnhammer EL. 2001. Predicting transmembrane protein topology with a hidden Markov model: application to complete genomes. J Mol Biol. 305: 567–580.

Lavrov DV, Forget L, Kelly M, Lang BF. 2005. Mitochondrial genomes of two demosponges provide insights into an early stage of animal evolution. Mol Biol Evol. 22:1231–1239.

Lavrov DV, Lang BF. 2005a. Poriferan mtDNA and animal phylogeny based on mitochondrial gene arrangements. Syst Biol. 54:651–659.

Lavrov DV, Lang BF. 2005b. Transfer RNA gene recruitment in mitochondrial DNA. Trends Genet. 21:129–133.

Lévi C. 1957. Ontogeny and systematics in sponges. Syst Zool. 6:174–183.

Lévi C. 1964. Ultrastructure de la larve parenchymella de démosponge. I: *Mycale contarenii*. Cah Biol Mar. 5:97–104.

Lobry JR. 1996. Asymmetric substitution patterns in the two DNA strands of bacteria. Mol Biol Evol. 13:660–665.

Lowe TM, Eddy SR. 1997. tRNAscan-SE: a program for improved detection of transfer RNA genes in genomic sequence. Nucleic Acids Res. 25:955–964.

Löytynoja A, Milinkovitch MC. 2001. SOAP, cleaning multiple alignments from unstable blocks. Bioinformatics. 17:573–574.

Maldonado M. 2004. Choanoflagellates, choanocytes, and animal multicellularity. Invertebr Biol. 123:1–22.

Marck C, Grosjean H. 2002. tRNomics: analysis of tRNA genes from 50 genomes of Eukarya, Archaea, and Bacteria reveals anticodon-sparing strategies and domain-specific features. RNA. 8:1189–1232.

Martin W, Stoebe B, Goremykin V, Hapsmann S, Hasegawa M, Kowallik KV. 1998. Gene transfer to the nucleus and the evolution of chloroplasts. Nature. 393:162–165.

Medlin L, Elwood HJ, Stickel S, Sogin ML. 1988. The characterization of enzymatically amplified eukaryotic 16S-like rRNA-coding regions. Gene. 71:491–499.

Muricy G, Diaz MC. 2002. Order Homosclerophorida Dendy, 1905, Family Plakinidae Schulze, 1880. In: Hooper JNA, Van Soest RWM, editors. Systema Porifera: a guide to the classification of sponges. New York: Kluwer Academic/Plenum Publishers. p. 71–82.

Muricy G, Pearse JS. 2004. A new species of Oscarella (Demospongiae: Plakinidae) from California. Proc Calif Acad Sci. 55:600–614.

Nichols SA. 2005. An evaluation of support for order-level monophyly and interrelationships within the class Demospongiae using partial data from the large subunit rDNA and cytochrome oxidase subunit I. Mol Phylogenet Evol. 34:81–96.

Okimoto R, Macfarlane JL, Wolstenholme DR. 1990. Evidence for the frequent use of TTG as the translation initiation codon of mitochondrial protein genes in the nematodes, *Ascaris suum*

and *Caenorhabditis elegans*. Nucleic Acids Res. 18:6113–6118.
Pearson WR. 1994. Using the FASTA program to search protein and DNA sequence databases. Methods Mol Biol. 25:365–389.
Robertus JD, Ladner JE, Finch JT, Rhodes D, Brown RS, Clark BF, Klug A. 1974. Structure of yeast phenylalanine tRNA at 3 A resolution. Nature. 250:546–551.
Ronquist F, Huelsenbeck JP. 2003. MrBayes 3: Bayesian phylogenetic inference under mixed models. Bioinformatics. 19:1572–1574.
Saghai-Maroof MA, Soliman KM, Jorgensen RA, Allard RW. 1984. Ribosomal DNA spacer-length polymorphisms in barley: mendelian inheritance, chromosomal location, and population dynamics. Proc Natl Acad Sci USA. 81:8014–8018.
Shao Z, Graf S, Chaga OY, Lavrov DV. 2006. Mitochondrial genome of the moon jelly *Aurelia aurita* (Cnidaria, Scyphozoa): a linear DNA molecule encoding a putative DNA-dependent DNA polymerase. Gene. 381:92–101.
Sonnhammer EL, von Heijne G, Krogh A. 1998. A hidden Markov model for predicting transmembrane helices in protein sequences. Proc Int Conf Intell Syst Mol Biol. 6:175–182.
Staden R. 1996. The Staden sequence analysis package. Mol Biotechnol. 5:233–241.
Strimmer K, von Haeseler A. 1996. Quartet puzzling: a quartet maximum likelihood method for reconstructing tree topologies. Mol Biol Evol. 13:964–969.
Thompson JD, Higgins DG, Gibson TJ. 1994. CLUSTAL W: improving the sensitivity of progressive multiple sequence alignment through sequence weighting, position-specific gap penalties and weight matrix choice. Nucleic Acids Res. 22:4673–4680.
Tyler S. 2003. Epithelium—the primary building block for Metazoan complexity. Integr Comp Biol. 43:55–63.
Van Soest RWM. 1984. Deficient *Merlia normani* Kirkpatrick, 1908, from the Curaçao reefs, with a discussion on the phylogenetic interpretation of sclerosponges. Bijdr Dierkd. 54: 211–219.
Wolstenholme DR. 1992. Animal mitochondrial DNA: structure and evolution. Int Rev Cytol. 141:173–216.
Woollacott RM, Pinto RL. 1995. Flagellar basal apparatus and its utility in phylogenetic analyses of the Porifera. J Morphol. 226:247–265.
Yen MR, Tseng YH, Nguyen EH, Wu LF, Saier MHJ. 2002. Sequence and phylogenetic analyses of the twin-arginine targeting (Tat) protein export system. Arch Microbiol. 177:441–450.

Franz Lang, Associate Editor

Accepted October 27, 2006